

ON THE FRETTING FATIGUE BEHAVIOR OF QUENCHED AND TEMPERED STEEL IN SMOOTH POINT CONTACT

A. PASANEN¹, A. LEHTOVAARA^{1*}, R. RABB², P. RIIHIMÄKI¹

¹ Department of Mechanics and Design, Tampere University of Technology
P.O. Box 589, 33101 Tampere, Finland

² Research & Development, Wärtsilä Finland Oy,
P.O.Box 244, 65101 Vaasa, Finland

* Corresponding author: Phone: +358 3 311511, Fax: +358 3 31152307,
Email: arto.lehtovaaara@tut.fi

ABSTRACT

Fretting fatigue can lead to a rapid decrease in the life of machine components when their contact surfaces have to transfer high tractions. Fretting fatigue was studied in partial, mixed and gross slip conditions made on quenched and tempered steel 34CrNiMo6. Measurements were made with sphere-on-plane contact geometry for smooth surfaces to detect macroscopic cracks. The fretting map type test series outlined a certain zone in partial and mixed slip conditions, where cracking occurred. The parameters affecting cracking threshold values and crack initiation are discussed.

Keywords; Fretting fatigue, fretting map, partial, mixed and gross slip, crack initiation

INTRODUCTION

Fretting may occur between any two contacting surfaces where short amplitude reciprocating sliding is present over a large number of cycles. This oscillatory movement can take place at the micrometer level, even without gross sliding of the contacting surfaces. This causes fretting wear of the surfaces and fretting fatigue, which can lead to a rapid decrease in fatigue life. The occurrence and severity of fretting fatigue is essentially dependent on the stress field on a contact (sub)surface caused by external bulk and contact loading. This stress field, affected by the oscillatory movement of the contacting surfaces, promotes crack nucleation. An extensive description of the fretting phenomenon and its associated contact mechanics is given in references [1- 3]. Fretting fatigue may cause hazardous and unexpected damage in machine components,

because the nominal stress levels occurring can be low and the damage initiated on the inside of the contact cannot be detected by normal visual inspection without opening the joint.

Both modelling and experiment are required to develop concise prediction methods and design rules for fretting fatigue. Numerical modelling of the fretting contact provides a detailed understanding of the stress field and the estimated cracking risk [4-6], whereas experimental fretting tests are very important in verifying the fretting fatigue models and in providing actual fretting wear and cracking data for design guidelines. The test results are most useful and informative when presented in the form of fretting maps, which describe the overall behaviour of fretting including contact conditions, the fretting regime, wear mechanism, crack nucleation and propagation [7]. The use of fretting maps was introduced

by Vingsbo et al. [8] and successively by, among others, Vincent et al. [9] in the form of running condition and material response fretting maps. Fouvry et al. [10] presented an advanced method for identifying the fretting regimes and the local friction coefficients based on the energy ratio and the sliding ratio.

Experimental fretting studies are often oriented towards particular cases with the advantage that the results can be related to that application. The disadvantage is that these results have often larger scatter and lack general applicability, because the contact conditions may not be well controlled and many parameters are varying at the same time. This disadvantage can be eliminated by using line and particularly point contact, which is important when fundamental fretting features are sought. The explicit equations governing pressure distribution and stress fields can also be found under these conditions [11, 12]. The vast majority of the experimental fretting studies have been conducted under gross sliding conditions, where the whole contact is sliding. However, fretting fatigue and corresponding crack formation is known to take place mainly in partial and particularly in mixed slip conditions. Fretting fatigue crack initiation for a point contact in controlled partial slip conditions has been systematically studied with bearing steel and titanium alloys [13, 14]. Crack location in the slip annulus and similar kinds of crack shapes were found in both studies. Line contact experiments in a partial slip regime with an aluminium alloy have shown that crack initiation appears sensitive to the surface quality with a higher roughness leading to a lower value of the tangential force needed for crack initiation [15]. The fretting fatigue and fatigue resistance of 34CrNiMo6 steel have been studied with elliptical contacts in gross slip conditions [16]. The improvement of fretting fatigue life with ion nitriding was observed.

However, little attention has been given to the fretting fatigue behaviour of quenched and

tempered 34CrNiMo6 steel, especially in the form of a fretting map. Quenched and tempered steel is a commonly used material in heavily loaded conditions, where the contact surfaces have to transfer high tractions. For example, in medium speed diesel engines this material is used in jointed components such as connecting rods, camshafts and crankshafts, where load conditions pose a potential risk of fretting.

This study focuses on the experimental characterization of fretting fatigue behaviour of quenched and tempered steel primarily in partial and mixed slip regimes with smooth point contact. The tests are organized using the fretting map concept with different normal load and tangential displacement amplitude levels. The number of load cycles required for crack initiation and the behavior of the tangential force and slip conditions during that time are also presented and discussed. In the future, this study provides a good opportunity for comparing observed results with calculated results subsequently derived from fretting model.

FRETTING POINT CONTACT

A sphere (body 1) and plane (body 2) make contact with the forces and coordinates as shown in Fig. 1.

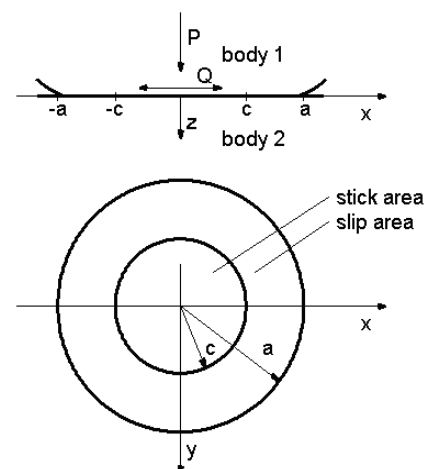


Figure 1. Schematic sphere-on-plane contact in partial slip condition.

Hertzian normal contact pressure distribution is assumed in elastic sphere-on-plane contact with smooth surfaces resulting in a Hertzian circular contact with radius a . The total normal force P in the z -direction is assumed to be constant ($P = P_o$), while the tangential force Q in the x -direction is oscillating with an amplitude of $\pm Q_o$. Once a tangential force is introduced, some sliding or at least partial slip between the contacting surfaces will occur. Assuming a constant friction coefficient μ over the slip zone, the radius of the stick zone c is given as [11]

$$c = a \left(1 - \frac{Q_o}{\mu P_o}\right)^{1/3} \quad (1)$$

The partial slip condition in the contact will occur when $Q < \mu P$. In this case, the surfaces in the central zone of the circular contact (bounded by stick radius c) will stick together whereas the outer zone will slip as shown in Fig. 1. If $Q = \mu P$ then the tangential force is at its maximum and gross sliding occurs between the surfaces. Running condition fretting maps have been introduced to locate the partial slip regime (PSR) and the gross slip regime (GSR) in the form of normal load versus relative tangential displacement. The transition between one slip regime and another defines the mixed slip regime (MSR). These slip regimes are known to have a strong effect on the material response in terms of no damage, cracking and wear as shown in Fig. 2.

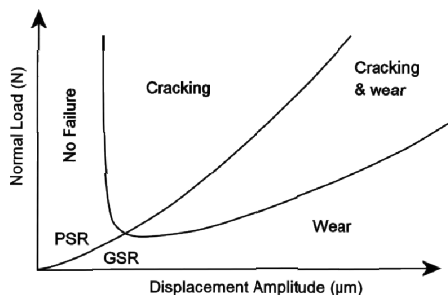


Figure 2. Schematic material response fretting map.

The partial slip regime near the gross slip regime and particularly the mixed slip regime have the highest cracking risk whereas clear gross slip conditions are more often related to excessive wear and debris formation. No damage is expected below a certain normal force level or for small displacement amplitudes. A knowledge of these thresholds is essential for designing so as to avoid fretting fatigue.

EXPERIMENTAL

A Hertzian point contact configuration with a sphere against a plane was used in the experiments. A detailed description of the test device is presented in reference [17]. The principle of the fretting test device is shown in Fig. 3 and a short overview is given below.

The test device has three similar sphere-on-plane test contacts running simultaneously. The plane is the test specimen, which can be loaded with a constant tension stress. The normal force on the pads with spherical contact profiles is generated by the hydraulic cylinder through the bearing and plate, which allows equal force distribution between the three contacts. The tangential displacement amplitude and the motion frequency, i.e. the reciprocating rotational motion of the test pads, can be adjusted and controlled accurately by the electric shaker control unit. The normal force, tangential force or displacement amplitude, and the bulk stress are adjusted and measured separately.

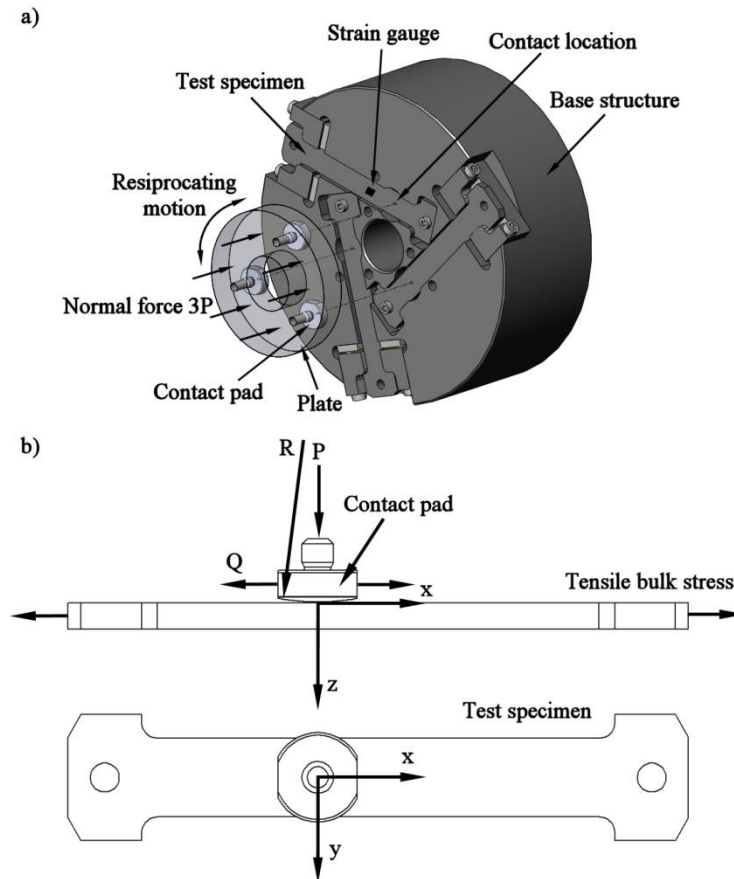


Figure 3. Principle of the test device.

The total tangential force induced by the three contacts with specified tangential displacement is measured continuously by the torque transducer integrated into the plate. The frictional force of the single contact can be obtained by dividing the total tangential force by the number of contacts. Tangential displacement is measured continuously from the relative movement between the fixed base structure of the specimen and the movable plate. This measured displacement includes possible sliding in contact together with compliance of the contact and test device. The strain gauge attached to every test specimen measures the bulk tensile stress, but this is also slightly affected by stress field variation resulting from crack growth. Changes in the stress trend provide an opportunity to identify the start and end points of crack growth. The calibration of the transducers was checked at regular intervals.

Test specimens

The contact pads and test specimens were made from quenched and tempered steel 34CrNiMo6. The spherical shapes of the pads were formed by grinding and polishing. The geometry and surface roughness of the contact pads were measured with a 3-D optical profilometer (Wyco NT 1100) for every test pad prior to the fretting fatigue tests. The measured spherical radii of the pads were 0.285 ± 0.015 m. The large radius of the sphere combined with reasonable contact pressure provided a contact area large enough for examination of crack location and of the slip zone regime.

Each test specimen has a width of 15 mm and a thickness of 5 mm. An example of the topography of the plane surface used in the tests is shown in Fig. 4.

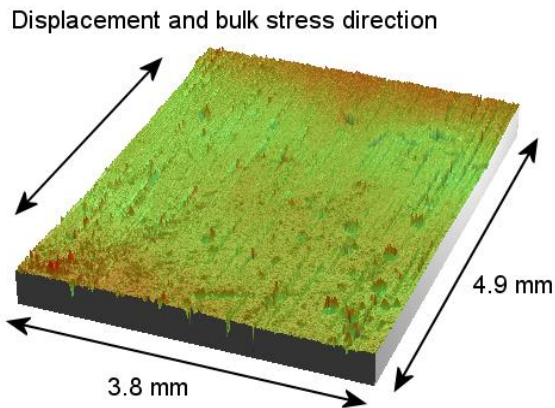


Figure 4. Polished surface of the test specimen.

The test specimens were polished to the same surface roughness as the test pads. The range of the measured surface roughness values of the test pads and the test specimens are presented in Table 1.

Table 1. Surface roughness of the test pads and the test specimens.

Contact body	Ra [μm]	Rt [μm]
Pad (sphere)	0.04-0.11	1.1-2.9
Specimen (polished)	0.04-0.11	1.1-2.9

The roughness of the test specimens was measured from the surface area of $3.8 \times 4.9 \text{ mm}^2$ consisting of eight separate measurements. R_a represents the roughness average, the arithmetic mean of the absolute value of the surface departures from the mean plane. All test specimens were polished at the same patch to obtain maximum similarity.

Test procedure

A constant bulk stress was applied to the test specimens, after which the normal load was applied. The test was started by increasing the tangential displacement amplitude linearly with automatic operation from zero to the target value during the first 5000 cycles. Carefully controlled amplitude increase is important at the beginning of the test to prevent gross sliding of the surfaces. The target amplitude was kept constant during the rest of the test. The test time was set to 19.5

hour, i.e. 2.8×10^6 cycles. The measured signals were saved to computer hard disc for further analysis. A hysteresis loop was created from the tangential force and displacement amplitude signals with a data collection frequency of 5000 Hz on each channel. This allows continuous follow-up of contact conditions during measurements. The measurements were carried out in the laboratory at room temperature. The contact surfaces were cleaned with solvent beforehand.

Test matrix

The basic idea was to carry out a series of tests, which may outline the earlier presented fretting map type behavior with different normal load and tangential displacement amplitude levels as shown in Table 2.

The load and amplitude levels were chosen according to results from preliminary tests, in which a suitable operating window was established by taking into account the boundaries of slip regimes as well as cracking and non-cracking regimes. The tensile bulk stress in the test specimens was set to 400 MPa in all tests. The frequency of the tangential motion was 40 Hz.

Friction coefficient

The contact slip regime conditions were followed continuously with the tangential force – displacement cycle, i.e. the hysteresis loop, which was measured on-line during the experiments with a data collection frequency of 5000 Hz on each channel. The area inside the hysteresis loop represents the work E_d done by the tangential force during the complete cycle and this energy is dissipated by reversed micro-slip in the slip zone $c \leq r \leq a$ [3]. The average of the hysteresis energy and the total energy E_t were calculated afterwards from a one second sample (40 load cycles) of measured data every 10 minutes during the test.

Table 2. Test matrix.

Surface	Normal force P [N]	Hertzian mean and (maximum) pressure (MPa)	Measured tangential displacement amplitude [μm] and contact condition (PSR=partial slip, MSR=mixed slip or GSR=gross slip)			
Polished	280	136 (204)	4,5 (GSR)	8,5 (GSR)		
Polished	680	183 (274)	6 (MSR)	8 (MSR)		
Polished	800	193 (289)	11 (MSR)	12 (MSR)		
Polished	1270	225 (337)	8 (PSR)	9 (PSR)	10,5 (MSR)	
Polished	2240	272 (408)	8 (PSR)	9 (PSR)	11 (PSR)	12,5 (PSR)

In sphere-on-plane contact operating in the partial slip regime, the friction coefficient can be obtained from equation 2, where A is the ratio of hysteresis energy and total energy, $A = E_d / E_t$ [10]:

$$A = \frac{6}{5} \frac{\left(1 - \left(1 - \frac{Q}{\mu P} \right)^{5/3} - \frac{5Q}{6\mu P} \left\{ 1 + \left(1 - \frac{Q}{\mu P} \right)^{2/3} \right\} \right)}{\frac{Q}{\mu P} \left\{ 1 - \left(1 - \frac{Q}{\mu P} \right)^{2/3} \right\}} \quad (2)$$

The friction coefficient μ in the slip zone is assumed to be constant. The tangential force amplitude Q and the normal force P were obtained from measurements. The point when the energy ratio A is 0.2 represents conditions where the contact condition changes to gross sliding.

In the gross slip regime, the friction coefficient is obtained by dividing the tangential force by normal force. The evaluation of the friction coefficient for quenched and tempered 34CrNiMo6 steel is presented and discussed in more detail in reference [18].

RESULTS AND DISCUSSION

Cracking behavior

The measurements were made with different load and tangential displacement levels including mostly partial and mixed slip conditions. Each test case included three

parallel pad-specimen test contacts under similar operating conditions. The results in the form of normal load versus relative tangential displacement amplitude with polished surfaces are shown in Fig. 5. The results for 0 crack means that during the test none of the three contacts was cracked whereas in a case of 3 cracks all of the three contacts were cracked. Only macroscopic cracks were counted (Fig. 7).

The slip conditions were determined from the energy ratio A defined in equation 2 and these are summarized in Table 2. Partial slip conditions exist at highest normal force level. This result was confirmed by post inspection of contact traces with the two shortest amplitudes where the cracking had not altered the contact trace. With a normal force level of 1270 N, the shortest amplitude test was carried out still just within the partial slip regime, whereas at the longest amplitude the test was in the mixed slip regime. The mixed slip condition starts with partial slip ($A < 0.2$) and during the test turns to gross sliding. Tests with force levels of 680 and 800 N were carried out in the mixed slip regime. The 680 N test case with the shortest amplitude provided an energy ratio of up to 0.2, whereas the 800 N test case with longest amplitude stayed in the partial slip regime only for a very short time at the beginning of the test and reached an energy ratio value of over 0.3 at the end of the test. The lowest normal force level 280 N was always in the gross slip regime.

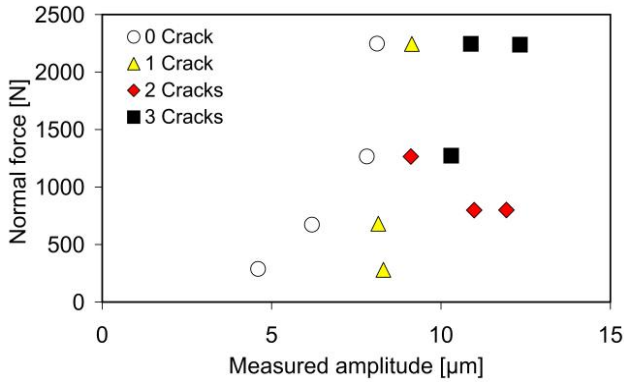


Figure 5. The measured material response fretting map for quenched and tempered steel with polished surfaces, $\sigma_{bulk} = 400$ MPa, Table 2.

The results in Fig. 5 outline the region where cracking mainly takes place. The heavy cracking occurs with partial and especially in mixed slip regimes bounded by certain normal force and tangential displacement amplitude limits, which are very important values for design purposes. No cracking was found even at the highest force level if the amplitude is short enough in the partial slip regime. The threshold for the normal force is not precisely established because, at the lowest force level, one contact of the six tested included the cracking. The boundary derived from the measured results agrees well with the fretting map concept discussed earlier.

In measurements under operating conditions where cracking is just appearing, only one or two test contacts out of three may have cracks. This supports the view of the statistical nature of (fretting) fatigue behaviour. The result where all three test contacts have cracks indicates that the operating conditions are clearly in the cracking region. In fact, the test case with highest load and longest amplitude already had two cracks in all three contacts at both trailing edges. This statistical behaviour results in the scatter of the cracking / no cracking boundary.

The theoretical tangential displacement amplitude based on the measured tangential

force and friction coefficient indicates a shorter amplitude than the corresponding measured one due to the compliance of the test device. This may also mean that at different load levels the share of tangential displacement caused by test device compliance varies and this may disturb the measured boundary line between cracking and no cracking. This can be eliminated by presenting the results in a form of normal force versus tangential force amplitude as shown in Fig. 6. Moreover, the tangential force has a major effect on the shear stress amplitude in the contact surface which is one of the key parameters for characterization of the initiation of fretting cracks [19]. In the measurements, the tangential displacement amplitude was kept constant during the test allowing variation of the tangential force caused by the possible changes in friction or contact conditions. The effective tangential force amplitude presented Q_{eff} is the mean value calculated from the beginning of the test to the mean crack initiation time in each test. This effective mean value is believed to reflect the tangential force, which is the essential factor in crack initiation. The tangential force after the crack has been initiated may no longer be as relevant due to the changes in contact conditions. In the test cases, where all three specimens were non-cracked, the mean value of the tangential force covered the whole test period.

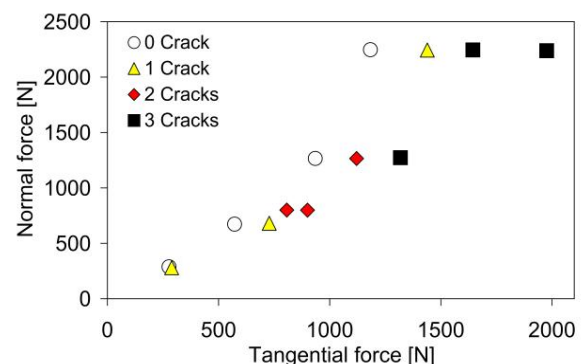


Figure 6. Fretting contact cracking behavior presented as normal force versus effective tangential force amplitude for quenched and tempered steel with polished surfaces, $\sigma_{bulk} = 400$ MPa, Table 2.

The boundary between cracking and no cracking is shown clearly in Fig. 6. This shows that the threshold tangential force for crack initiation is dependent on the normal force. At each normal load level the cracking risk, i.e. the number of cracks, increases as the tangential force amplitude increases towards the upper limit μP , which is reached at the beginning of the gross slip regime. The results also show that the effective friction coefficient in the fretting contact has been very high. In mixed and gross slip conditions, this can be estimated to be Q_{eff}/P resulting in a value of over 1.0, which already causes very high traction forces. Calculation of the stress field at the contact surface revealed that the maximum von Mises stresses at the highest load and amplitude levels are already in the range of yield stress of the test material.

Crack shape and initiation time

The fretted contact traces and cracks were studied with microscopic examination of test specimens as shown in Fig. 7a.

Each of the three test contacts during one test showed similar kinds of wear tracks. The shape of the crack stayed fairly constant under different load conditions, being a smoothly curved macroscopic crack. The initiation of the crack took place near the edge of the contact in the slip direction ($x/a = \pm 1$, $y/a = 0$). This is the location where the calculated cracking risk has its maximum value [4]. The formation of a crack in the early stages often causes extra wear outside the initial contact area around the crack and disturbs the stick zone as discussed in [17]. The length of the crack is larger than the contact diameter. One specimen (Fig. 7a) with a representative macroscopic crack was cut in the middle of the contact in the slip direction and its cross section at A-A is shown in Fig. 7b. The crack started to grow smoothly inwards into the contact. This kind of crack shape is typical when using a constant bulk stress [20]. In this specimen, the depth of the macroscopic crack is about 3 mm.

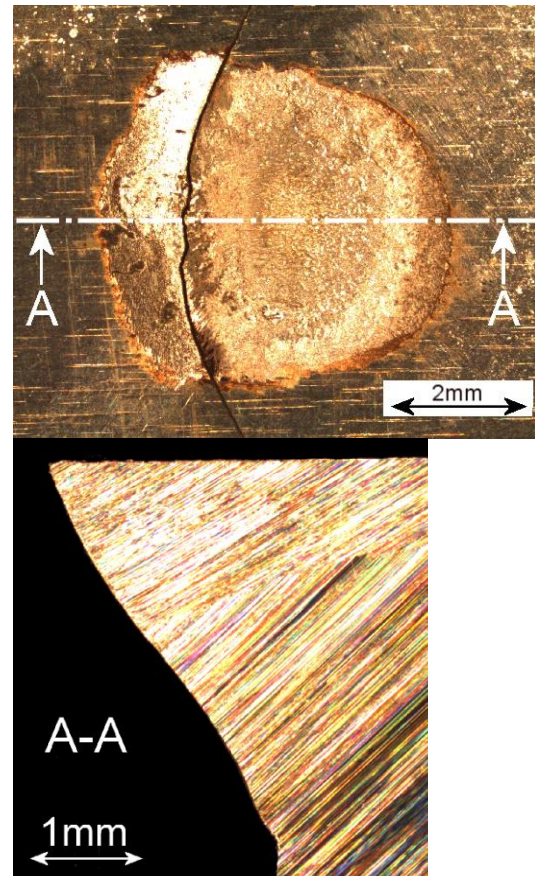


Fig. 7. Fretting contact trace with one crack and the gross section at A-A. Oscillation motion occurred in a vertical direction and initially in the partial slip regime, $P = 2245$ N, $\delta = 11$ μ m.

It was clear that some contacts also involved rupture-like (micro) cracks, where the nature and location was different from the macro cracks described in Fig. 7.

The number of load cycles required for macro crack initiation and the growth of the crack was estimated from strain-gauge measurements near the fretting contact as shown in Fig. 3. The strain-gauge measures the tensile bulk stress, but it is also slightly affected by the stress field variation caused by crack growth. This trend in the stress change provides an opportunity to identify the start and end times of crack growth. Typical results of tensile stress behavior as a function of time are presented in Fig. 8.

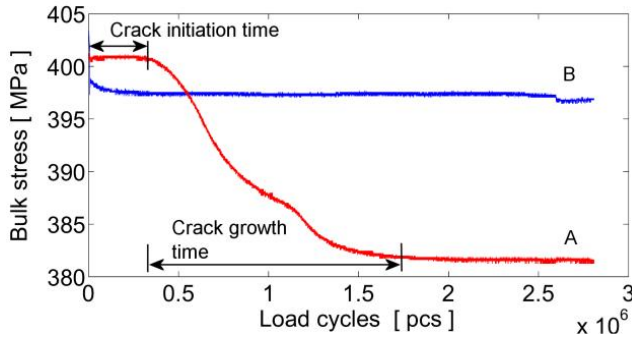


Figure 8. Behavior of tensile stress near the fretting contact during the test (A – cracks, B – no cracks).

Fig. 8 shows that the bulk tensile stress is almost constant and equal to the bulk stress value set initially. After a certain number of load cycles, the stress in the test specimen A starts to decrease rapidly, indicating that crack growth has started. After a defined number of load cycles the stress value stabilizes, indicating that crack growth has ceased as is expected with constant bulk stress. The measured stress drop, though small, is in most cases clear and logically predictable. The measured strain-gauge signals were analyzed using this method and the results are shown in Fig. 9.

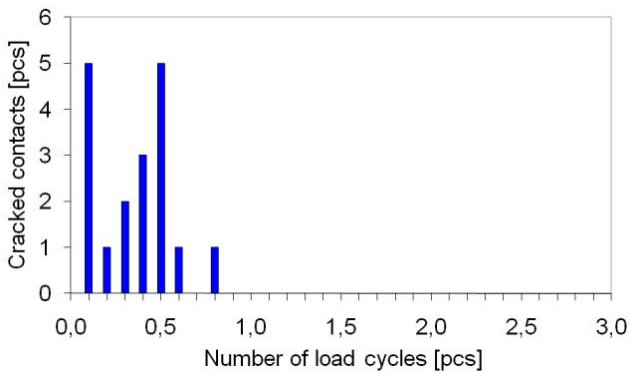


Figure 9. The distribution of the crack initiation times

Fig. 9 shows that the crack initiation typically starts in a range of 0.1 – 0.6 million load cycles with a maximum of 0.8 million cycles. The scatter is large as would be expected because of different kinds of load conditions and also because of statistical nature of the phenomenon. The mean crack initiation time, used in conjunction with the effective

tangential force, is a mean value of the three crack initiation times obtained from each test. The non-cracked specimens were not included in this mean value. It is obvious that the shortest crack initiation time corresponds to almost instant initiation of the crack, because it may take some time for the crack to become large enough to be detected by strain gauges.

Traction time dependence

The on-line energy method allowed subsequent examination of the trend of the instant friction coefficient as well as the instant tangential force during the measurements. The crack initiation time was also monitored with strain-gauges. This offers the possibility of studying the interactions between these parameters so as to gain some insight into crack initiation conditions. The tangential displacement amplitude and the normal force were kept constant during the tests. The friction coefficient μ , the ratio of the tangential force to the normal force (Q_o/P) and the energy ratio A as a function of load cycles are shown in Fig. 10. The crack initiation times (t_{c1} and t_{c2}) are included in the figure. The friction coefficient and tangential force are obtained by calculating their mean value during one second (40 cycles) every 10 minutes.

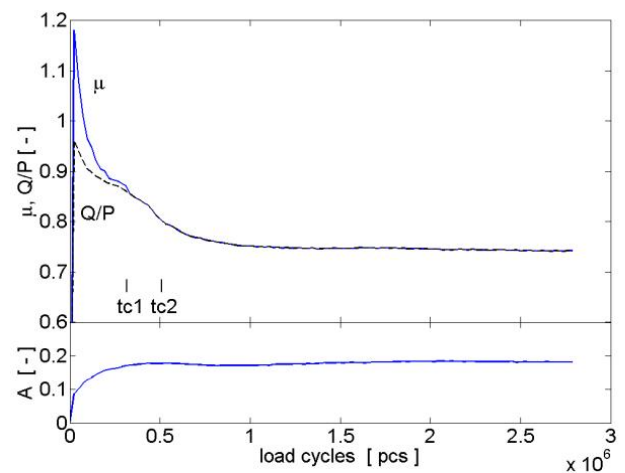


Figure 10. Friction coefficient μ , Q_o/P -ratio and energy ratio A as a function of load cycles, $P = 1265 \text{ N}$, $p_o = 338 \text{ MPa}$, $\delta = 9 \mu\text{m}$.

Fig. 10 shows that the friction coefficient and tangential force have their maximum value just after the displacement amplitude has been automatically raised to a constant speed at the target value during the first 5000 load cycles. At this stage, the contact is considered to be in the partial slip regime due to the low value of the energy ratio and the clear difference in the friction coefficient and the Q_o/P -ratio. After 5000 load cycles, the test continues with a constant tangential displacement amplitude. The friction coefficient, the tangential force and their difference decreases and the energy ratio increases, indicating that fretting contact conditions are moving towards gross slip, obviously due to the wearing of the contact. At load cycle $0.3E6$ the friction and Q_o/P -ratio are equal and continue to decrease until they settle at a constant value. The energy ratio also settles to a constant value at around the same time. The crack initiation times reveal that crack initiation is closely related to a high local friction coefficient and tangential traction values at the beginning of the test. The friction peaks can also be found in the non-cracked test cases, which eliminate the possibility that the decrease of friction and tangential force is solely due to the crack initiation and growth.

The magnitude of the friction coefficient peak at the beginning of the test seems to be dependent on the operating parameters employed. The trend is that the friction peak is small in the test cases with short amplitude and the peak increases with increasing displacement amplitude towards the mixed slip regime in tested normal force levels.

CONCLUSIONS

Fretting fatigue was studied in partial, mixed and gross slip conditions using quenched and tempered steel 34CrNiMo6 applying a fretting

map concept. Measurements were made with sphere-on-plane contact geometry with polished surfaces. Only macroscopic cracks with particular shapes and location were counted, and these can be seen by microscopic examination of the contact trace without breaking the specimen. The following conclusions were drawn:

- The fretting map type test series, using different normal force and displacement amplitude or tangential force levels defined a certain zone in partial and mixed slip conditions, where cracking occurred. Threshold tangential force for crack initiation is dependent on the normal force.
- Crack initiation is greatly influenced by the tangential force amplitude peak at the beginning of the test after the displacement amplitude has been increased steadily to the target value. The appearance of this force peak is promoted by operation in a mixed slip zone.
- The statistical nature of fretting fatigue behaviour was observed using three similar test contacts running simultaneously. These may result in cracking in one, two or three contacts, which expands the validity of the results.

ACKNOWLEDGEMENTS

This study is a part of a FREFA (Fretting Fatigue in Diesel Engineering) research project. The authors are grateful for the financial support provided by Wärtsilä Finland Oy and the Finnish Funding Agency for Technology and Innovation.

NOMENCLATURE

a	= radius of Hertzian contact (m)
A	= energy ratio (-)
c	= contact stick radius (m)
E_d	= hysteresis energy (J)
E_t	= total energy (J)
p_o	= maximum Hertzian pressure (Pa)
P, P_o	= normal force (N)
q	= tangential traction in the x-direction (Pa)
Q	= tangential force (N)
Q_{eff}	= effective tangential force amplitude (N)
Q_o	= tangential force amplitude (N)
R	= sphere radius of contact pad (m)
Ra	= surface roughness (μm)
Rt	= surface roughness, peak-to-peak value (μm)
t_c	= crack initiation time (load cycles)
x	= coordinate along sliding direction
y	= coordinate normal to sliding direction
z	= depth coordinate
σ_{bulk}	= external bulk stress in the x-direction (Pa)
δ	= measured tangential displacement amplitude (m)
μ	= friction coefficient (-)

REFERENCES

- [1] Waterhouse, R.B. (Ed), Fretting Fatigue, Applied Science Publishers, Barking, 1981, p. 244.
- [2] Hills, D.A., Novell, D., Mechanics of Fretting Fatigue, Dordrecht, Kluwer Academic Publishers, 1994, p. 236.
- [3] Johnson, K.L., Contact Mechanics, Cambridge University Press, 1985, p. 452.
- [4] Lehtovaara, A., Rabb, R., A numerical model for the calculation of fretting fatigue crack initiation for a smooth spherical contact, Finnish J. of Tribology, 25 (2006) 23-30.
- [5] Lehtovaara, A., Rabb, R., Fretting fatigue crack initiation for a smooth spherical contact – a parameter study, Finnish J. of Tribology, 25 (2006) 31-40.
- [6] Lehtovaara, A., Rabb, R., A numerical model for the evaluation of fretting fatigue crack initiation in rough point contact, Wear 264 (2008) 750-756.
- [7] Zhou, Z.R., Nakazawa, K., Zhu, M.H., Maruyama, N., Kapsa, Ph., Vincent, L., Progress in fretting maps, Tribology International 39 (2006) 1068-1073.
- [8] Vingsbo, O., Söderberg, S., On fretting maps, Wear 126 (1988) 131-147.
- [9] Vincent, L., Berthier, Y. and Godet, M. "Testing methods in fretting fatigue: a critical appraisal" ASTM STP 1159, 1992, pp. 33-48.
- [10] Fouvry, S., Kapsa, Ph., Vincent, L., Developments of fretting sliding criteria to quantify the local friction coefficient evolution under partial slip condition, Tribology Series 34 (1998) 161-172.
- [11] Mindlin, R. D., Compliance of elastic bodies in contact, J. Appl. Mech. 16 (1949) 259-268.
- [12] Hamilton, G. M., Explicit Equations for the Stresses beneath a Sliding Spherical Contact, Proc Instn Mech Engrs Vol 197C, 1983, 53-59.
- [13] Alfredsson, B., Cadario, A., A study on fretting friction evolution and fretting fatigue crack initiation for a spherical contact, Int. J. Fatigue 26 (2004) 1037-1052.
- [14] Kuno, M., Waterhouse, R.B., Nowell, D., Hills, D.A., Initiation and growth of fretting fatigue cracks in the partial slip regime, Fatigue and Fracture of Eng. Mater. and Structs, 12 (1989) 387-398.

[15] Proudhon, H., Fouvry, S., Buffière, J.-Y., A fretting crack initiation prediction taking into account the surface roughness and the crack nucleation process volume, *Int. J. Fatigue* 27 (2005) 569-579.

[16] Costa, J.D., Ferreira, J.M. and Ramalho, A.L, Fatigue and fretting fatigue of ion-nitrided 34CrNiMo6 steel, *Theoretical and Applied Fracture Mechanics* 35 (2001) 69-79.

[17] Pasanen, A., Järvisalo, S., Lehtovaara, A., Rabb, R., Development of a test device for the evaluation of fretting point contact, *Lubrication Sci.* 21 (2009) 41-52.

[18] Pasanen, A., Lehtovaara, A., Rabb, R., and Riihimäki, P., Friction behavior of quenched and tempered steel in partial and gross slip conditions in fretting point contact, *Wear* (2009), doi:10.1016/j.wear.2009.03.047.

[19] Fellows, L.J., Nowell, D., Hills, D.A, On the initiation of fretting fatigue cracks, *Wear* 205 (1997) 120-129.

[20] Cadario, A Alfredsson, B. Fretting fatigue crack growth a spherical indenter with constant and cyclic bulk load. *Engineering Fracture Mechanics* 72 (2005) 1664-1690.